

**MARS POLAR COLD SPOTS OBSERVED BY MRO/MARS CLIMATE SOUNDER.** P. Hayne<sup>1</sup>, D. A. Paige<sup>1</sup>. <sup>1</sup>University of California, Los Angeles (595 Charles Young Blvd E, Los Angeles, CA 90095; phayne@ucla.edu)

**Introduction:** Using radiometric observations from the Mars Climate Sounder (MCS) during southern winter, we report evidence that polar cold spots ( $T_b < 135$  K) at Mars' south pole are correlated with tropospheric, optically thick clouds. In limb observations coincident with nadir measurements of low brightness temperature regions, clouds appear as radiation sources at typical altitudes of 20 – 30 km. Using statistical methods, we confirm that transient cold spots appearing during polar night are correlated with the presence of clouds above the surface, which are likely composed of CO<sub>2</sub> ice. Areas where cold spots persist over the full range of solar longitude are also characterized by persistent clouds, the thickness of which is inversely correlated with nadir brightness temperature. We model the Mars south polar night atmosphere with a customized delta-Eddington code, including spherical geometry in the formal solution to the equation of radiative transfer. By forward-modeling a multi-layered atmosphere, we attempt to reproduce the MCS radiance data. Emission, absorption, and scattering by gas, dust, and ice (CO<sub>2</sub> and H<sub>2</sub>O) clouds are all included in the model. Surface emissivity, as well as cloud optical thickness, composition, and altitude are constrained by comparison of the MCS data with the model output.

**Theories of Cold Spot Origins:** Since their discovery during the Viking era, radiometrically cold areas (“cold spots” below the CO<sub>2</sub> equilibrium temperature of  $\approx 148$  K at surface pressures) within the polar regions during the polar night have remained an enigma. Three primary explanations have been explored previously [1]:

(1) *Depletion of atmospheric CO<sub>2</sub>:* Condensation of carbon dioxide could lead to enrichment in non-condensable phases, lowering  $P_{CO_2}$  and allowing lower equilibrium surface temperatures [2].

(2) *Non-unit emissivity of surface CO<sub>2</sub>:* Formation of frost or freshly condensed snow could lower the emissivity of the surface [3].

(3) *Carbon dioxide clouds:* Optically-thick CO<sub>2</sub> clouds could result in lower measured brightness temperatures due to scattering and/or low temperature blackbody emission [4, 5].

Hess [6] demonstrated that (1) is feasible only under special circumstances due to dynamical instability. The spectral properties of CO<sub>2</sub> frost and clouds are similar such that it has been difficult to discriminate between (2) and (3) as viable hypotheses. In the pre-

sent investigation, we use radiance measurements of both the atmospheric limb and nadir to better constrain the possible origin of the polar cold spots.

**Observations of Cold Spots:** The Mars Climate Sounder [6] onboard the Mars Reconnaissance Orbiter (currently in orbit at Mars) recorded a series of nadir and limb radiance measurements in nine spectral channels, from  $\sim 1$ – $40$   $\mu\text{m}$  wavelength. The observations used in this study spanned a range of solar longitude,  $L_s = 111$  to 148, corresponding to southern winter. Radiances are converted to equivalent brightness temperatures using the radiometric response function of each filter and the Planck function. Observations are binned by latitude and longitude ( $1$ – $5^\circ$  bins) and  $L_s$ , and nadir brightness temperatures are compared to measured limb brightness temperature profiles. Figure 1 shows an example of the correlation between clouds and nadir cold spots.

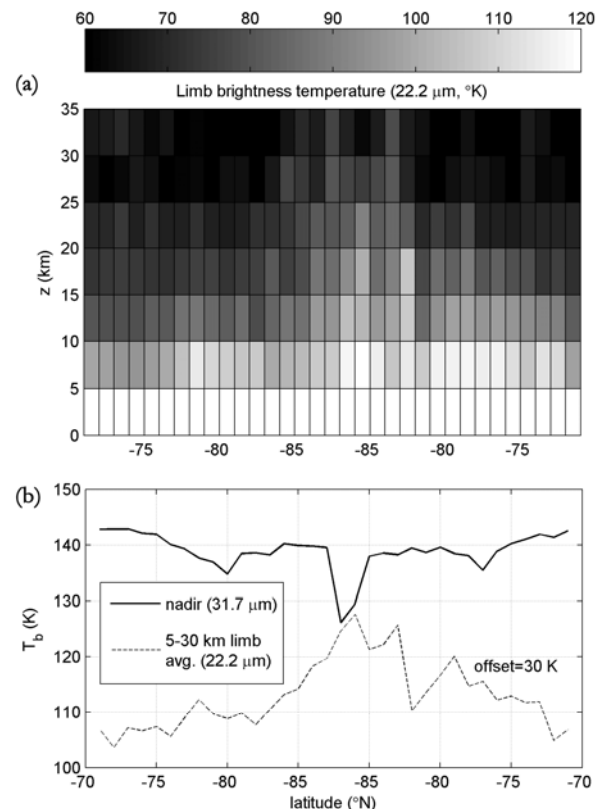


**Figure 1.** (a) MCS limb brightness temperature vs. latitude for the South Polar region on a single orbit during polar night. (b) Correlation of nadir (solid line) and limb (dashed line) brightness temperatures.

**Data Analysis:** We plotted limb brightness temperature profiles for the A5 channel ( $22.2\ \mu\text{m}$ ) for areas where measured nadir brightness temperatures (within three degrees of  $L_s$ ) dropped below 137 K (or 140 K) in the B1 ( $31.7\ \mu\text{m}$ ) channel. Figure 2a compares these limb profiles (blue; shaded area indicates  $1\sigma$ ) to measurements at the same location, but during the period of maximum temperature for that spatial bin (red). During the period when the cold spot is present in the nadir data, brightness temperatures rise significantly at  $\sim 20\text{--}30\ \text{km}$  altitude. This is interpreted as a cloud, whose brightness temperature in the nadir may be indicative of the altitude of optical depth  $\sim 1$ , several kilometers above the surface. Figure 2b shows the location of the cold spots for each of the two cutoff temperatures.

Statistical analysis shows that the  $22\text{-}\mu\text{m}$  brightness temperatures at  $\sim 30\ \text{km}$  altitude are inversely correlated ( $R=-0.55$ ,  $p<10^{-14}$ ) with nadir  $32\text{-}\mu\text{m}$  brightness temperatures (Fig. 2). A thorough analysis was performed to exclude any field-of-view effects due to

surface radiance. We therefore conclude that the systematic increase in limb radiance is due to the presence of optically-thick clouds, likely composed of  $\text{CO}_2$  ice particles.

**Modeling:** The  $\delta$ -Eddington approximation of the radiative transfer equation (RTE) incorporates a forward peak into the Eddington phase function, accurately representing asymmetric scattering by aerosols. Monochromatic fluxes can be calculated rapidly using this approximation within each layer of an  $N$ -layer atmosphere, given appropriate boundary conditions and optical properties of each layer. Once these fluxes have been calculated for each MCS spectral channel, we integrate the formal solution to the RTE along a desired ray path. This calculation yields the predicted MCS brightness temperature spectrum, given the properties of the model atmosphere and viewing geometry. Cloud height and composition are free parameters in this iterative scheme, which results in an accurate representation of the south polar nighttime atmosphere and surface properties. Preliminary results will be pre-

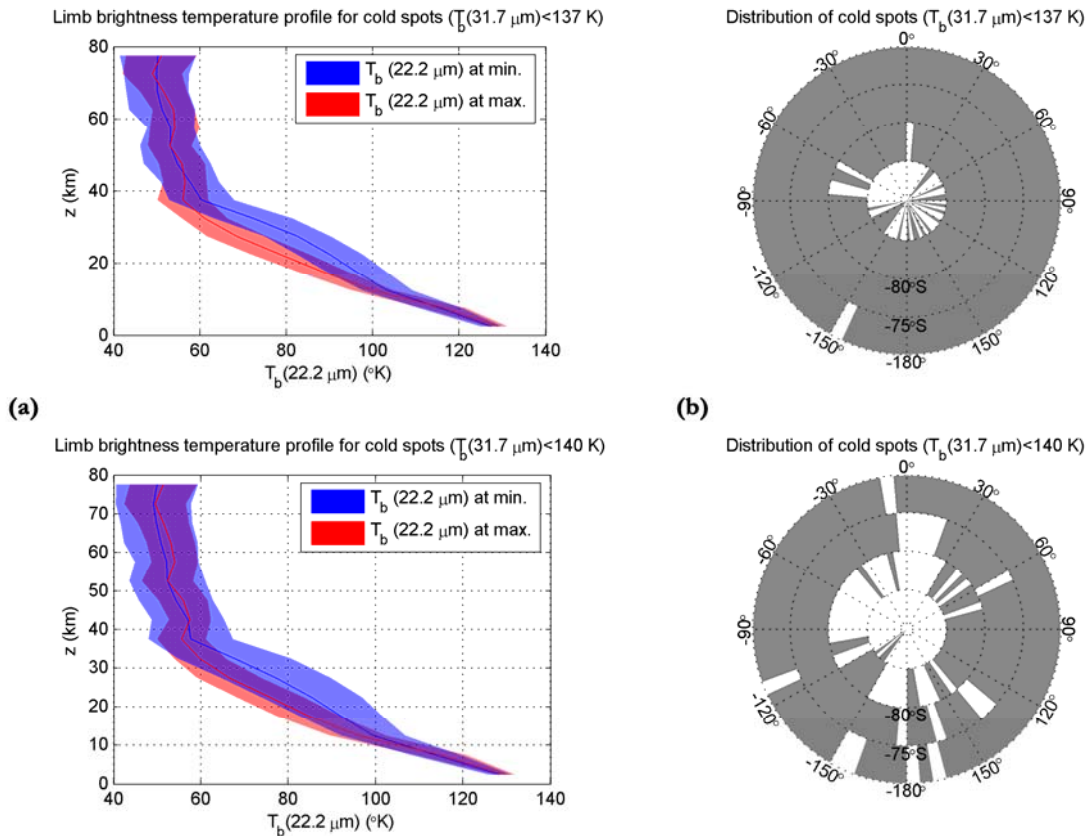


**Figure 2.** (a) MCS  $22.2\text{-}\mu\text{m}$  brightness temperature profiles for south polar cold spots during their warmest (red) and coldest (blue) as viewed in the nadir, for two different  $T_b$  thresholds (top= $137\ \text{K}$ ; bottom= $140\ \text{K}$ ). Note the increase in  $T_b$  around  $25\ \text{km}$  during the cold periods. (b) The distribution of south polar cold spots (white) for the two threshold temperatures.

sented at this meeting.

**Discussion and Future Work:** Our statistical analysis shows that the brightness temperatures of polar cold spots viewed from above correlate well (inversely) with the presence of clouds viewed at the limb. As discussed by other authors [1], this observation does not rule out the possibility of surface emissivity effects playing a significant role as well. Our radiative transfer model will lend insight into the origin of cold spots and their role in the polar nighttime atmosphere. Tropospheric CO<sub>2</sub> clouds may persist throughout polar night (see Figure 3), precipitating carbon dioxide snow particles and adding latent heat to the polar thermal balance. Dust may also play a significant role in the origin and evolution of CO<sub>2</sub> clouds and the associated cold spots. Implications for the global energy balance and seasonal deposition of carbon dioxide will also be explored.

**References:** [1] Forget et al. (1995) *JGR* 100, 21,219. [2] Kieffer et al. (1977) *JGR* 82, 4,249. [3] Dittion and Kieffer (1979) *JGR* 84, 8294. [4] Hunt (1980) *GRL* 7, 481. [5] Paige et al. (1990) *Bull. Am. Astron. Soc.* 22, 1075. [6] Taylor, F. W. et al. (2006) *Adv. in Space Res.* 38, 4, 713-717.

**Acknowledgement:** Tim Schofield provided useful comments related to this work.

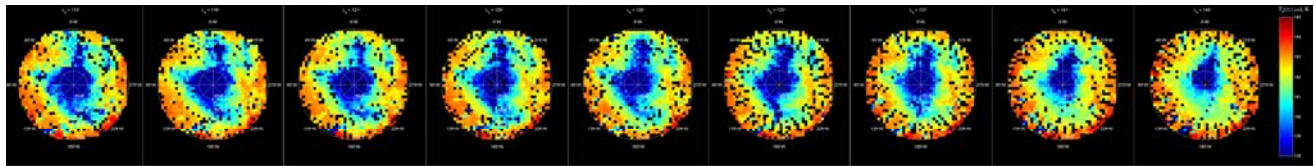


**Figure 3.** Distribution of polar cold spots (blue shades) over the south polar winter. The first frame is  $L_s = 111^\circ$  and the last is  $145^\circ$ .